ORGANIC PROCESS RESEARCH & DEVELOPMENT
OPR&D
Article
pubs.acs.org/OPRD

RP-HPLC DAR Characterization of Site-Specific Antibody Drug Conjugates Produced in a Cell-Free Expression System

Yiren Xu, Guifeng Jiang, Cuong Tran, Xiaofan Li, Tyler H. Heibeck, Mary Rose Masikat, Qi Cai, Alexander R. Steiner, Aaron K. Sato, Trevor J. Hallam, and Gang Yin*

Sutro Biopharma, Inc. 310 Utah Avenue, Suite 150, South San Francisco, California 94080, United States

Supporting Information

ABSTRACT: Antibody drug conjugates (ADCs) harness the target specificity of a monoclonal antibody (mAb) and the high cytotoxicity of a small molecule, enabling improved delivery of a potent antitumor agent compared to traditional chemotherapy for cancer therapy. Only two ADCs have been marketed, both of which are produced via nonsite-specific conjugation of the cytotoxic drug to either interchain cysteine (Adcetris) or lysine (Kadcyla). A growing body of evidence suggests that site-specific ADCs, because of their payload homogeneity, will improve pharmacokinetics and have wider therapeutic windows when compared to heterogeneous ADCs. Previously, we have demonstrated the use of a cell free expression system (Xpress CF+) for rapid production of site-specific ADCs. Here we report the generation of a variety of ADCs via conjugation between a site-specific incorporated non-natural amino acid (nnAA), *para*-azidomethyl-L-phenylalanine (pAMF), and dibenzocyclooctyl-(polyethylene glycol)$_4$ (DBCO-(PEG)$_4$) linked payloads using this platform. We developed a reversed phase HPLC method for drug to antibody ratio (DAR) characterization, which is applicable to both reduced and intact ADCs. We demonstrate that these ADCs are of near complete conjugation and exhibit potent cell killing activity and in vitro plasma stability. Moreover, we generated an ADC conjugated at both light and heavy chains, resulting in a DAR close to 4. With the increased number of payloads, the resultant DAR 4 ADC is potentially more efficacious than its DAR 2 counterparts, which could further improve its therapeutic index. These studies have demonstrated the competency of Xpress CF+ for site-specific ADC production and improved our understanding of the site-specific ADCs in general.

INTRODUCTION

The first generation of antibody drug conjugates (ADCs) were realized via drug conjugation on wild-type amino acids such as lysines[1] and reduced interchain cysteines,[2,3] which results in a distribution of cytotoxic drugs over many different sites of the ADC.[4,5] As a consequence, the heterogeneous product mixture has shown to have a narrow therapeutic index that is the amalgamation of different species with different efficacy and safety profiles.[6−8] On the other hand, the drug conjugation in site-specific ADCs is only through precise incorporated or modified handles, such that the drug to antibody ratio (DAR) and drug distribution can be controlled.[4,5,9] This control allows for the careful querying and optimization of important drug properties such as potency, pharmacokinetics, and safety.[6,10−13]

The first site-specific ADC to be exemplified was THIOMAB, which was achieved by engineering additional cysteines for drug conjugation.[10] With a DAR of 2, the homogeneous THIOMAB exhibits improved efficacy as well as in vivo stability compared to its heterogeneous ADC control with a DAR of 3.5 from heterogeneous conjugation—ultimately giving rise to a widened therapeutic window. Inspired by THIOMAB, tremendous endeavors have followed, mostly focusing on how to introduce the site-specific handle for conjugation. A variety of approaches have demonstrated successful applications in site-specific ADC generation, which have been comprehensively summarized in multiple reviews.[4,9,14] The primary categories include: (1) non-natural amino acid (nnAA) incorporation by utilizing stop (amber or opal) codon or four-base codons (e.g., *p*-acetophenylalanine (pAcF),[15] p-azidophenylalanine (pAzF),[16] *p*-azidomethylphenylalanine (pAMF)[17] and Pcl (pyrroline-carboxy-lysine)),[18] (2) enzymatic conjugation via recognition of a consensus sequence (e.g., transglutaminase[19] and formylglycine-generating enzyme[20]), and (3) manipulation of glycan[21,22] or interchain cysteines in the native antibody.[23−25]

Previously, we have established Xpress CF+, an in vitro transcription/translation system using *E. coli* based extract, for rapid production of site-specific ADCs containing pAMF.[17] Cell free expression systems are recognized for their high manipulability, productivity, and scalability in protein production.[26−28] It also has advantages over cell based expression systems for site-specific ADC generation, especially when using amber codon suppression for nnAA incorporation.[9,14,29] First, the open nature of cell free expression system yields unimpeded access of the nnAA to the enzymes required for its incorporation, which can be problematic in cellular systems due to poor cell membrane permeability. Second, as the amber codon is naturally recognized by release factor 1 (RF1) for translation termination, it is crucial to suppress the RF1 function in order to facilitate high-level nnAA incorporation in site-specific ADCs.[30] Unfortunately, the RF1 attenuation is complicated due to its essentiality in cell viability, such that it requires extensive strain engineering to fulfill this task in cell based expression systems.[31,32] In contrast, cell free expression systems offer a simple solution to this challenge by taking

Received: March 4, 2016
Published: May 31, 2016

DOI: 10.1021/acs.oprd.6b00072
Org. Process Res. Dev. 2016, 20, 1034−1043

advantage of the fact that the cell free protein synthesis is in fact decoupled from the cell growth.[33−35] In Xpress CF+, the function of RF1 is preserved during cell growth, and then deactivated prior to protein production, which is achieved by engineering an OmpT (outer membrane aspartyl protease) recognizable sequence into RF1 to trigger OmpT cleavage of RF1 upon the lysis of the cell wall.[14]

Though site-specific ADCs have a much simplified composition, they still require stringent control during manufacturing to ensure batch-to-batch consistency. Among a variety of properties, DAR and drug distribution are the quality attributes responsible for determining the efficacy and safety of ADCs.[5,36] Methods developed for conventional ADCs can be easily adapted for site-specific ADCs as well. Mass spectrometry (MS) has been widely used for ADC characterization such as ESI-TOF-MS[36−38] and less popular MALDI-TOF-MS,[39−41] based on the absolute mass shift upon conjugation. Except for ADCs conjugated via interchain cysteines,[42] MS can simultaneously quantify DAR and drug distribution of ADCs. Given that many payloads are highly hydrophobic, another commonly used analytical tool is chromatographic separation based on hydrophobicity, such as hydrophobic interaction chromatography (HIC),[43,44] and reversed phase (RP) chromatography.[36,45,46] Typically, HIC is performed on intact ADCs under nondenaturing condition, while RP is applied to reduced ADCs under denaturing condition to overcome its relatively low resolution.[47,48] Alternatively, other approaches are available depending on the chemistry of the linker and drug. For instance, imaged capillary isoelectric focusing (icIEF) has been reported to successfully separate lysine-conjugated ADCs, because conjugation on lysine eliminates the basic primary amine and consequently decreases the pI of the antibody.[36,49] Another method is the application of UV/vis spectroscopy for DAR analysis, which relies on differences in the maximal absorbance (A_{max}) between the drug and the antibody.[36,50]

Here we report the use of Xpress CF+ for the production of a variety of site-specific ADCs, the molecular diversity of which comes from different conjugation sites, different payloads, and a combination of both. We also developed a reversed-phase HPLC method and confirmed that the employed azide/alkyne copper-free click chemistry is capable of yielding ADCs with near complete conjugation. These cell-free produced site-specific ADCs exhibit high potency in cell killing as well as high stability in plasma. Moreover, we generated a site-specific ADC conjugated at both light chains (LC) and heavy chains (HC), resulting in a DAR close to 4. The DAR 4 site-specific ADC provides the possibility to further improve the therapeutic index due to the higher potency. These studies have demonstrated the competency of Xpress CF+ for site-specific ADC production and improved our understanding of the site-specific ADCs in general.

MATERIALS AND METHODS

Materials. Tris(2-carboxyethyl) phosphine (TCEP) was purchased from Thermo Scientific (Waltham, MA). *para*-Azidomethyl-L-phenylalanie (pAMF) and all payloads were synthesized by ACME bioscience (Palo Alto, CA), including dibenzocyclooctyl-(polyethylene glycol)$_4$-monomethyl auristatin F (DBCO-PEG$_{(4)}$-MMAF), dibenzocyclooctyl-(polyethylene glycol)$_4$-valine-citrulline-monomethyl auristatin E (DBCO-PEG$_{(4)}$-vc-MMAE), and dibenzocyclooctyl-(polyethylene glycol)$_4$-emtansine (DBCO-PEG$_{(4)}$-maytansinoid). Horseradish peroxidase (HRP) conjugated goat antihuman Fc was purchased from Jackson ImmunoResearch Laboratories (West Grove, PA). Tetramethyl benzidine substrate was purchased from KPL (Gaithersburg, ML). Cell Titer-Glo reagent was purchased from Promega Corp. (Madison, WI).

Protein Engineering. Using site-directed mutagenesis, amber codon (TAG) was engineered into the wild type trastuzumab HC or LC at the selected sites for conjugation. They are S7 and T22 in LC (Kabat numbering), S136, R355, N389, and F404 in HC (EU numbering) (Figure 1).

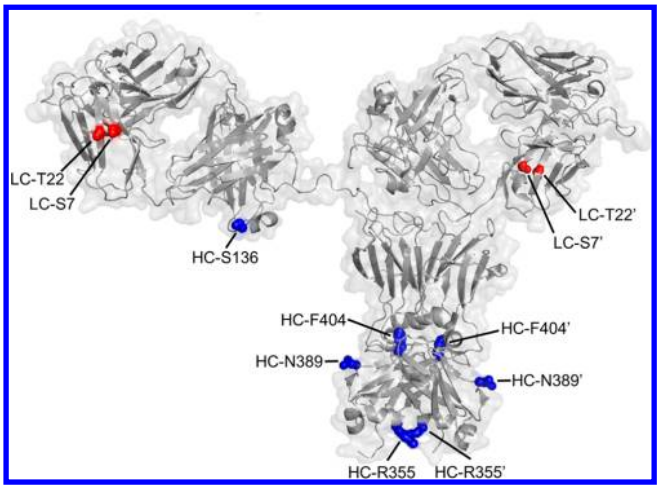

Figure 1. Positions of conjugation sites on a human IgG1 (1HZH) as an illustrative example.[60] All six residues selected for pAMF incorporation shown here are conserved in trastuzumab. Two LC positions are labeled in red, and four HC positions are labeled in blue. One of the HC-S136 is not shown due to the lack of defined structure in the crystal.

Cell-Free Protein Expression and Purification. Cell-free protein expressions were performed as previously described with the following modifications.[17] A mixture of extract SBEZ023 and SBDG108 was used at a ratio of 15% to 85%, where SBEZ023 contains amber suppressor tRNA[17] and SBDG108 contains chaperones required for antibody folding and assembly.[51] To reduce potential mis-incorporation and promote pAMF incorporation, the concentrations of phenylalanine and tyrosine in the cell-free reactions were reduced to 0.5 mM, while pAMF was included at 2 mM in the cell free reactions. tRNA^{pAMF} synthetase was added exogenously at 2.5 μM. Similar to natural trastuzumab (WT), the expressions of these trastuzumab-derived site-specific ADCs were carried out at a ratio of 3:1 for HC:LC plasmids at a total of 10 μg/mL (4 nM).[52] Expressions were set up at 30 °C overnight in thin-film Petri dish format without shaking. The pAMF-containing antibodies were purified as previously described.[17] The purity was >90%, evaluated by SDS-PAGE. The fidelity of pAMF incorporation and payload conjugation were confirmed by LC-MS as previously described.[17]

Drug Conjugation. Purified trastuzumab-derived variants containing pAMF were conjugated to three well-established microtubule disrupting agents, MMAF, MMAE, and maytansinoid (Chart 1).

The cytotoxic moieties are attached to a DBCO-PEG$_{(4)}$ linker, enabling copper free click chemistry between the azide group on pAMF and the alkyne from DBCO for antibody-drug conjugation.[53] In detail, 5 mM stock solution of the payloads in DMSO was mixed with 2−3 mg/mL of purified pAMF

DOI: 10.1021/acs.oprd.6b00072
Org. Process Res. Dev. 2016, 20, 1034−1043

Chart 1

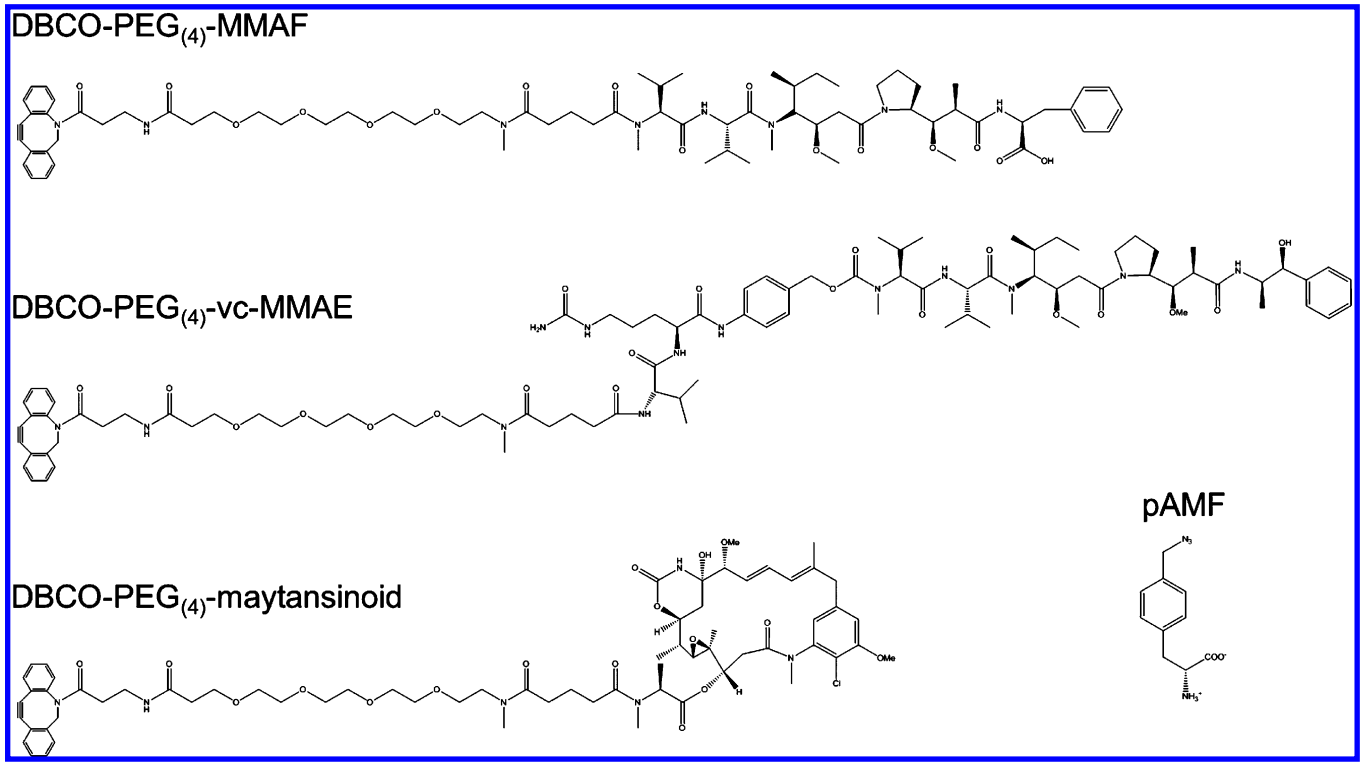

containing antibodies at a drug to antibody molar ratio of 10:1 for overnight incubation at room temperature. To prepare the partially conjugated ADCs, the drug and antibody was mixed at a ratio of 1:1. Mixtures with various drug:antibody ratios from 1:4 to 10:1 were also prepared in order to identify the minimal drug requirement for complete conjugation. Lastly, the ADCs were prepared at drug:antibody ratio of 6:1, and samples were taken at 0.5, 1, 2, 3, 4, 5, 6, 7, and 20 h and quenched with sodium azide at a final concentration of 0.1 M.

DAR Determination. Reduced samples were prepared as follows: 2−3 mg/mL of ADCs in PBS was diluted to 0.5 mg/mL in 7.2 M guanidine-HCl, 0.3 M sodium acetate, pH 5.3, and reduced by addition of TCEP at a final concentration of 10 mM. The mixture was incubated at 37 °C for 15 min in an Eppendorf Thermomix R while shaking at 300 rpm. For intact samples, ADCs were diluted to 1 mg/mL in PBS. Both reduced and intact RP-HPLC analysis was performed on a Proteomix column (5 μm, 1000 Å, 2.1 × 150 mm from Sepax Technologies, Newark, DE), connected to an Agilent 1200 HPLC system containing a binary gradient pump, temperature-controlled column compartment, autosampler, and a diode array detector. The system ran at 0.5 mL/min at 80 °C using 0.1% trifluoroacetic acid (TFA) in water (mobile phase A, MPA) and 0.1% TFA in acetonitrile (ACN) (mobile phase B, MPB), and absorbance was monitored at 280 nm (reference wavelength at 360 nm). The DAD detector was set at 0.02 min for peak width, 1.6 Hz for data acquisition, and 0.12 s for time constant. A total of 2 μg of sample (either reduced or intact) was injected into the system and eluted with a 20 min method consisting of a 1 min isocratic hold at 30% MPB, a 14 min linear gradient from 30% to 45% MPB, a 3 min wash using 95% MPB, and last a 2 min re-equilibration at 30% MPB.

DAR can be characterized using both reduced and intact RP-HPLC methods. For reduced method, DAR was determined using eq 1 for ADCs with LC conjugation and eq 2 for HC conjugation, respectively (Figure S1):

$$\mathrm{DAR}^{\mathrm{LC}} = 2 \times \frac{\text{Peak Area of Conjugated LC}}{\text{Peak Area of Unconjugated LC} + \text{Peak Area of Conjugated LC}} \quad (1)$$

$$\mathrm{DAR}^{\mathrm{HC}} = 2 \times \frac{\text{Peak Area of Conjugated HC}}{\text{Peak Area of Unconjugated HC} + \text{Peak Area of Conjugated HC}} \quad (2)$$

As reduction results in HC/LC and HC/HC dissociation, the reduced method measures the single chains of HC or LC in either unconjugated or conjugated states. Therefore, DAR of the intact antibody is twice the fractional conjugation of the respective individual chain.

For the ADC conjugated on both LC and HC, $\mathrm{DAR}^{\mathrm{Total}}$ is the sum of $\mathrm{DAR}^{\mathrm{LC}}$ and $\mathrm{DAR}^{\mathrm{HC}}$ (eq 3):

$$\mathrm{DAR}^{\mathrm{Total}} = \mathrm{DAR}^{\mathrm{LC}} + \mathrm{DAR}^{\mathrm{HC}} \quad (3)$$

The intact RP-HPLC method measures the populations of unconjugated species (DAR0), one drug species (DAR1), and two drugs species (DAR2). Their corresponding peak areas are used in eq 4 to obtain $\mathrm{DAR}^{\mathrm{Total}}$:

$$\mathrm{DAR}^{\mathrm{Total}} = 1 \times \frac{\text{Peak Area of DAR1}}{\text{Total Peak Areas of DAR0, DAR1, and DAR2}} + 2 \times \frac{\text{Peak Area of DAR2}}{\text{Total Peak Areas of DAR0, DAR1, and DAR2}} \quad (4)$$

DOI: 10.1021/acs.oprd.6b00072
Org. Process Res. Dev. 2016, 20, 1034−1043

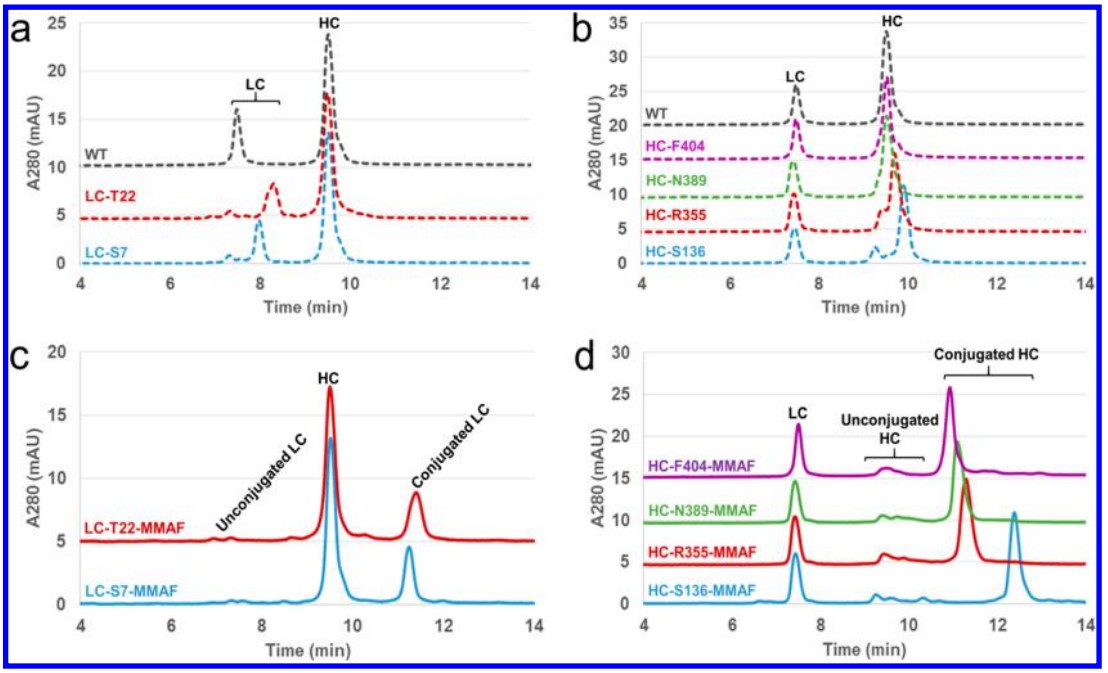

Figure 2. Xpress CF+ produced site-specific ADCs exhibit different hydrophobicity upon pAMF incorporation and MMAF conjugation. As shown in the RP-HPLC chromatograms of the reduced, unconjugated, and conjugated antibodies, pAMF incorporation at different positions on LC (a) and HC (b) increases hydrophobicity of the impacted chains compared to WT (gray dashed lines). MMAF conjugation further raises the hydrophobicity of the influenced LC (c) and HC (d). The extent of hydrophobicity change depends on the incorporation position.

DAR determination by LC-MS was performed as an orthogonal method to RP-HPLC and followed the procedure as described previously.[17]

In Vitro Plasma Stability. The ADC was incubated at 100 μg/mL in PBS, human plasma, cynomolgus monkey plasma, mouse plasma, and rat plasma for 5 min, 1 d, 2 d, 3 d, 4 d, and 7 d. When harvesting, 100 μL of streptavidin magnetic beads were coated with either 10 μg of biotin-HER2-ECD (extracellular domain and binding target for trastuzumab) for human plasma incubation or biotin-anti-hFc for all other plasma incubations and then mixed with 100 μL of plasma samples. For DAR characterization, the bead captured ADC was released from the magnetic beads by incubation in 25 μL of 1% TFA for 5 min at room temperature. The mixture was then spun in a desktop centrifuge. The supernatant was prepared for the reduced RP-HPLC analysis as described above.

HER2 ECD ELISA. To measure total IgG concentration in plasma samples, 96-well ELISA plates were coated with 0.5 μg/mL HER2 ECD in carbonate/bicarbonate buffer (pH 9.6) at 4 °C overnight. After removal of the coat solution, nonspecific binding sites were blocked with blocking solution [0.5% bovine serum albumin (BSA) in PBS] for 1−2 h at room temperature. The plates were then washed with washing buffer (0.05% Tween in PBS), and the standards or samples diluted in ELISA assay buffer [PBS containing 0.5% BSA, 0.05% Tween, 10 ppm proclin 300, 0.2% bovine g-globulin, 0.25% CHAPS, 0.35 M NaCl, 5 mM EDTA (pH 7.4)] were added. After 2 h of incubation, plates were washed, and HRP conjugated goat antihuman Fc was added and incubated at room temperature for additional 2 h. Plates were then washed again, followed by the addition of tetramethyl benzidine substrate for color development. The reaction was stopped after 10−15 min by the addition of 1 M phosphoric acid. Plates were read on a Molecular Devices microplate reader at a wavelength of 450 nm. The concentration of IgG in the samples was extrapolated from a four-variable fit of the standard curve.

Cell Cytotoxicity Assay. Cytotoxicity effects of the conjugated trastuzumab variants on cells were measured with a cell proliferation assay. SKBR3 cells (a total of 10^3 cells per well) were seeded in a volume of 40 μL in a 96-well half area flat bottom white polystyrene plate. The cells were allowed to adhere overnight at 37 °C in a CO_2 incubator. ADC variants were formulated at 2× concentration in DMEM/F12 medium and filtered through MultiScreen HTS 96-Well Filter Plates (Millipore; Billerica, MA). Filter sterilized, conjugated, or unconjugated trastuzumab variants were added into treatment wells, and plates were cultured at 37 °C in a CO_2 incubator for up to 7 days. For cell viability measurement, 80 μL of Cell Titer-Glo reagent was added into each well, and plates were processed as per product instructions. Relative luminescence was measured on an ENVISION plate reader (PerkinElmer; Waltham, MA). Relative luminescence readings were converted to % viability using untreated cells as reference. Data were fitted with nonlinear regression analysis, using log (inhibitor) vs response, variable slope, four-parameter fit equation on GraphPad Prism (GraphPad v 5.00, Software; San Diego, CA). Data were expressed as % relative cell viability vs dose of ADC in nM.

RESULTS

Conjugation Sites. A total of six trastuzumab-derived site-specific ADCs were selected for this study, where the codon corresponding to LC-S7, LC-T22, HC-S136, HC-R355, HC-N389, and HC-F404 was replaced by an amber codon for pAMF incorporation, respectively (Figure 1). These sites were among the top-ranked positions based on their performance in amber codon suppression, conjugation efficiency, and potency in a previous screening effort of many solvent-accessible residues in trastuzumab IgG.[9,14,29] The pAMF-containing

DOI: 10.1021/acs.oprd.6b00072
Org. Process Res. Dev. 2016, 20, 1034−1043

antibodies were expressed at 0.5−1 L scale in the thin film format.[52]

For this study, the six pAMF containing trastuzumab-derived variants were conjugated to DBCO-PEG$_{(4)}$-MMAF, DBCO-PEG$_{(4)}$-vc-MMAE, and DBCO-PEG$_{(4)}$-maytansinoid via copper free click chemistry. To simplify the nomenclature, the unconjugated antibodies were denoted by their pAMF position such as HC-F404, while the names of the corresponding ADCs were extended to include the drug name such as HC-F404-MMAF.

Hydrophobicity Increase in Antibodies upon pAMF Incorporation. pAMF is a hydrophobic nnAA, the incorporation of which induces a demonstrable hydrophobicity increase of the antibody. In the reduced RP-HPLC chromatograms, there are two main peaks observed within the gradient for these unconjugated pAMF containing antibodies, corresponding to LC and HC. Compared to WT trastuzumab without pAMF, LCs and HCs with pAMF are clearly right-shifted (Figure 2a−b). Interestingly, the extent of hydrophobicity change varies depending on the position of pAMF. Between the two pAMF containing LCs, LC-T22 appears to be more hydrophobic than LC-S7 (Figure 2a). pAMF incorporation has different degrees of effect on the HC hydrophobicity as well, with a descending order of hydrophobicity from HC-S136, HC-R355, HC-N389 to HC-F404 (Figure 2b).

In addition to the main peaks, we also observed a small peak in front of the pAMF containing LC or HC peaks. These minor peaks elute closely but not exactly at the retention time for WT LC or HC (Figure 2a−b). These species presumably are product related impurities. For DAR determination, as these minor species are unable to be conjugated with drugs, their corresponding peaks are categorized under "unconjugated" LCs or HCs. Therefore, the DAR values reported by RP-HPLC may be slightly underestimated due to the presence of minor impurities.

High DARs for Xpress CF+ Produced Site-Specific ADCs. The three drugs used in the experiments, MMAF, MMAE, and maytansinoid, are all highly hydrophobic. Therefore, the resultant ADCs exhibit increased hydrophobicity upon drug conjugation. In the reduced RP-HPLC chromatograms of LC conjugates, the conjugated LCs are further shifted to the right, while the unconjugated LCs remain unshifted. The same phenomenon was observed for HC conjugates, but with a lesser degree of a retention time shift, likely due to the relatively larger size and already inherent longer retention time of the HC as compared to the LC. We generally observed at least two peaks in the regions of the unconjugated species (Figure 2c−d). They may come from (1) unconjugated species due to kinetic barriers given that the drugs were supplied in great excess; and (2) impurities coeluting with either unconjugated LCs or HCs.

Like pAMF incorporation, drug conjugation also has differential impacts on the hydrophobicity of ADCs among the variants tested. For LC conjugates, LC-T22-MMAF appears to be slightly more hydrophobic than LC-S7-MMAF (Figure 2c). However, the difference between the two LC conjugates (Δ = 0.16 min) is smaller than that between the two pAMF containing LCs (Δ = 0.33 min), suggesting that the conjugated drug dominates the hydrophobicity of the conjugated LCs. Among four HC conjugates, the same trend of hydrophobicity was observed for these HC conjugates as for their unconjugated counterparts (Figure 2d). Surprisingly, the order of the hydrophobicity of these pAMF containing HCs, as well as their corresponding MMAF conjugates, happens to be in alignment with the pAMF incorporation position in the sequence. The closer to the N-terminus the incorporated pAMF is located for drug conjugation, the more hydrophobic the resultant pAMF containing antibody and ADC are. Whether this correlation has an underlying structural reason is unclear, and requires examination of more sites on multiple antibodies. Due to the limited number of LC conjugates in this study, no trend could be deduced yet.

Using peak areas from the reduced RP-HPLC method, we confirmed high DAR values for all six site-specific ADCs. For instance, MMAF conjugation yields DARs ranging from 1.67 to 1.89 (Table 1). MS analysis was performed as an orthogonal approach and produced comparable results (Table 1 and S1). As MS based DAR determination uses the information on DAR0, DAR1, and DAR2 species only, there is no interference from product-related or nonproduct related impurities. On the other hand, RP-HPLC relies on the chromatographic resolution of each species, and uses peak areas for DAR calculation. Therefore, the subtle discrepancy in DAR values acquired by these two different approaches is likely due to impurities, as well as the inherent variabilities of the respective methods. When site-specific ADCs with high purity were analyzed, matching DAR values could be obtained using RP-HPLC and LC-MS.

Table 1. DARs Obtained by Different Methods

	drug	reduced RP	intact RP	LC-MS
LC-S7	MMAF	1.84	1.71	1.79
	MMAE	1.84	1.57	
	maytansinoid	1.92	1.79	
LC-T22	MMAF	1.89	1.73	1.82
	MMAE	1.88	1.64	
	maytansinoid	1.93	1.79	
HC-S136	MMAF	1.72	1.64	1.72
	MMAE	1.62	1.47	
	maytansinoid	1.84	1.70	
HC-R355	MMAF	1.67	1.67	1.74
	MMAE	1.60	1.51	
	maytansinoid	1.71	1.77	
HC-N389	MMAF	1.71	1.76	1.80
	MMAE	1.67	1.61	
	maytansinoid	1.75	1.84	
HC-F404	MMAF	1.75	1.82	1.89
	MMAE	1.67	1.73	
	maytansinoid	1.84	1.86	

Besides MMAF, we also conjugated MMAE and maytansinoid onto these antibodies. The site-specific ADCs conjugated with MMAE or maytansinoid show the similar trend of the site-determined hydrophobicity change as with MMAF conjugation (Figure S2). The ADCs conjugated with MMAF, MMAE, and maytansinoid at the same position, however, exhibit different apparent hydrophobicities, resulting from the different hydrophobicities of these drugs (Figure 3). Comparison of the conjugation on the same site illustrates that maytansinoid conjugation yielded the highest DAR values among the three drugs, regardless of conjugation on the LC or HC, while MMAE conjugation resulted in the lowest DAR values, especially for the HC conjugates (Table 1).

MMAF and maytansinoid are attached to the same noncleavable linker, while MMAE is attached to a cleavable linker (Chart 1). As the same batch of pAMF containing

DOI: 10.1021/acs.oprd.6b00072
Org. Process Res. Dev. 2016, 20, 1034−1043

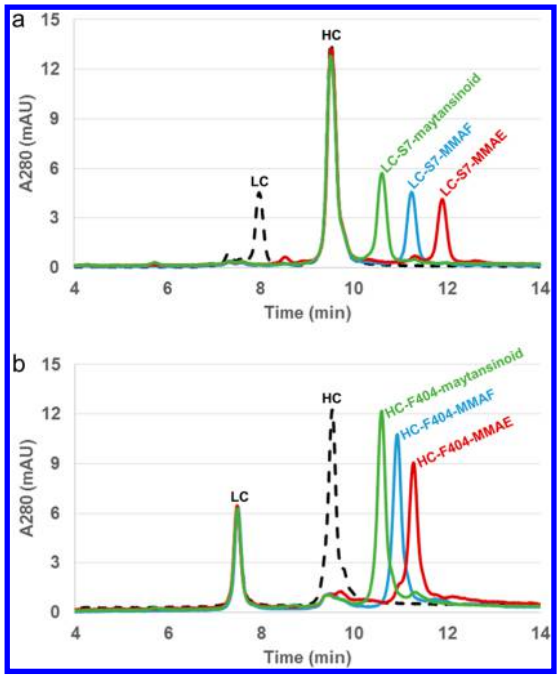

Figure 3. Hydrophobicity of site-specific ADCs is influenced by drug. The representative RP-HPLC chromatograms were acquired on LC-S7 (a) and HC-F404 (b) conjugated with MMAF (blue), MMAE (red), and maytansinoid (green), respectively. Compared to unconjugated species (black dashed line), the hydrophobicity of the conjugated LC or HC is significantly increased, the extent of which depends on the hydrophobicity of the drug per se.

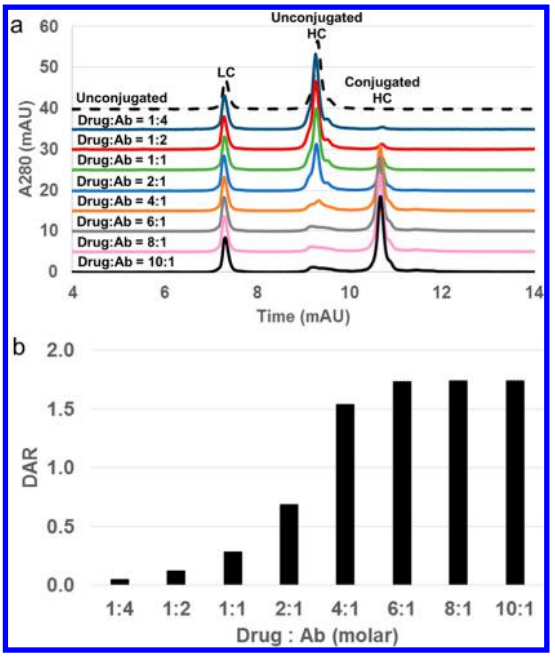

Figure 4. Drug-to-antibody ratio for complete conjugation. Using the reduced RP-HPLC method as a monitoring tool, (a) a range of drug–antibody molar ratios from 1:4 to 10:1 were used for MMAF conjugation on HC-F404. The conjugations were performed at room temperature overnight. Complete conjugation was observed at drug–antibody ratio of 6:1.

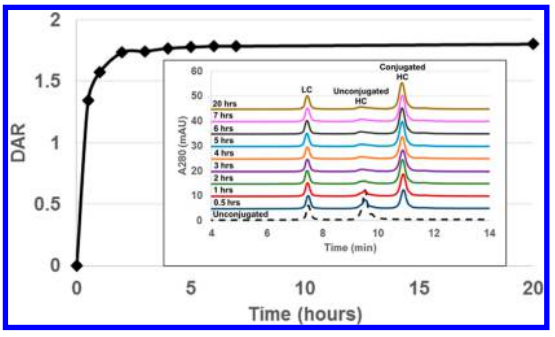

Figure 5. Conjugation kinetics of HC-F404-MMAF. At minimal drug–antibody ratio (6:1) required for complete conjugation, conjugation is complete within 2 h at room temperature. Conjugation beyond 2 h showed no changes in the RP-HPLC chromatography.

antibodies were used for conjugation, the slightly lower DARs of MMAF or MMAE conjugated ADCs may be due to the impurity of in payload stock solutions. Indeed, we discovered that the DBCO-$PEG_{(4)}$-MMAF stock contains several peaks on a HISEP column, indicating product impurities in the stock solution (data not shown). Though the identities of these impurities are not clear, we speculate that some species may still enable conjugation on pAMF of the antibodies, but lack part of, or entire highly hydrophobic moiety, which would reflect as "unconjugated" species in RP chromatograms, leading to lower DAR estimation. These outcomes might be readily prevented by using freshly prepared high-purity linker-drug stock for conjugation, designing a more stable drug-linker, and preserving the ADCs with appropriate formulation and storage condition.

Conjugation Efficiency. We typically used a drug–antibody molar ratio of 10:1 for conjugation. Though each antibody needs only two drugs to achieve complete conjugation theoretically, the reaction slows down with the decrease of the available reactants. Therefore, drugs are provided in excess to promote faster conjugation. However, it is more cost-effective and environmentally responsible to use the minimal amount of drug required to maintain the same conjugation efficiency. Thus, we examined a wide range of drug–antibody ratios from 1:4 to 10:1 for MMAF conjugation to HC-F404. With an overnight incubation at room temperature, the drug–antibody ratio of 6:1 and above delivered the same result as 10:1 (Figure 4).

Next, we investigated the kinetics of MMAF conjugation to HC-F404 at drug:antibody ratio of 6:1. The conjugation was >95% complete within 2 h (Figure 5). Longer incubation only yields a marginal increase in DAR. We also evaluated the conjugation kinetics at drug:antibody ratio of 10:1 and found that the additional excessive drug did not promote faster conjugation (data not shown).

Temperature is another important determinant of conjugation efficiency. The reaction is generally accelerated at higher temperature such as 30 °C or beyond and decelerated at lower temperature. Considering that the antibodies may be more prone to degradation or aggregation under higher temperature, we performed all conjugation at room temperature, a trade-off between the conjugation efficiency and antibody integrity. As such, it is advantageous that efficient azide–alkyne conjugation can be achieved at neutral pH and room temperature, in comparison to other conjugations such as oxime-acetyl reaction, which is typically performed at 37 °C, pH 4.5 for 16–48 h.[15]

Exploring Site-Specific ADCs with DAR of 4. Furthermore, we generated a site-specific ADC with MMAF conjugation at both LC-S7 and HC-S136. Using the reduced

DOI: 10.1021/acs.oprd.6b00072
Org. Process Res. Dev. 2016, 20, 1034–1043

RP-HPLC method, LC-S7-MMAF yields DAR of 1.81 and HC-S136-MMAF DAR of 1.85, resulting in an additive DAR of 3.66 for the dual conjugated site-specific ADC (Figure 6). LC-MS

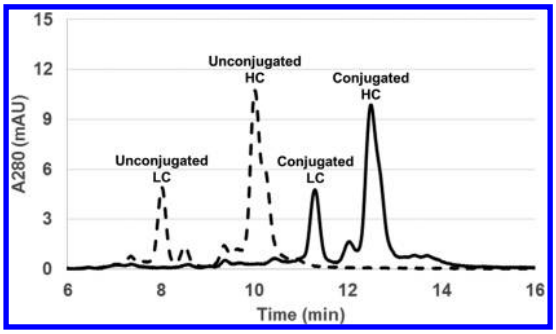

Figure 6. Xpress CF+ produced a site-specific ADC with MMAF conjugation on both LC and HC. Using the reduced RP-HPLC method, MMAF conjugation on LC exhibited DAR of 1.81, and MMAF conjugation on HC DAR of 1.85, respectively. Therefore, the additive DAR of the resultant site-specific ADC is 3.66.

analysis determined the DAR to be 3.52. As the drug load is doubled, this DAR4 site-specific ADC rendered an approximately half of EC_{50} value as its DAR2 controls (LC-S7-MMAF and HC-S136-MMAF) in the cell killing assay (Sutro proprietary data). Assuming the DAR4 site-specific ADC shares similar stability to its corresponding DAR2 ADCs, it would presumably widen the therapeutic window.[54]

Intact RP-HPLC. Previously, most published RP-HPLC methods were developed for ADCs with heterogeneous conjugation; it is critical to reduce the sample to separate HCs and LCs in order to overcome the relatively low resolution of RP-HPLC.[45,47,48] In the circumstance of site-specific ADCs, the sample composition is significantly simplified, making intact DAR characterization by RP-HPLC possible. However, no report has been published on this topic at the time of this writing. As such, we investigated if the developed RP-HPLC method is also competent to analyze intact ADCs. Using HC-F404-MMAF as an example, we observed three peaks with baseline resolution in the intact RP chromatogram, corresponding to unconjugated antibody (DAR0), antibody conjugated on one site (DAR1), and antibody conjugated on both sites (DAR2) (Figure 7). The identities of these species were confirmed using partially conjugated HC-F404-MMAF and by LC-MS (data not shown). To our knowledge, this is the first successful application of RP-HPLC in characterization of DAR

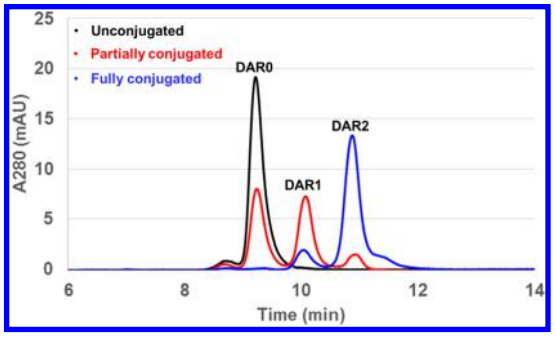

Figure 7. Intact DAR characterization by RP-HPLC. RP-HPLC chromatograms revealed baseline resolution of DAR0, DAR1, and DAR2 species for unconjugated (black), partially conjugated (red) and fully conjugated (blue) HC-F404-MMAF.

as well as drug distribution on the intact ADCs. In most cases, the intact RP-HPLC method reported slightly lower, but still comparable DAR values than the reduced RP-HPLC method (Table 1). Interestingly, these site-specific ADCs also clearly manifest varied hydrophobicity in the intact chromatograms, though no trend can be identified (Figure S3). It is noteworthy that a variety of RP columns have been inspected during intact DAR RP-HPLC method development, including commonly used Varian PLRP-S, C4, C8, and C18 columns (data not shown). The selected Proteomix column gave the best performance in the separation of DAR0, DAR1, and DAR2 species in site-specific ADCs. This intact RP-HPLC method is also quality control (QC) friendly and can serve as a release assay, as minimal sample preparation is needed leading to a robust analysis.

Cell Killing and in Vitro Plasma Stability of Xpress CF+ Produced Site-Specific ADCs. The 6 Xpress CF+ produced site-specific ADCs were conjugated to MMAF, MMAE, or maytansinoid and subjected to cell killing analyses using the HER2 positive breast cancer cell line SKBR3. All of them showed similar potency regardless of the conjugated drugs (Figure 8). The stability of the site-specific ADCs was assessed from the perspective of DAR and total protein. HC-F404-MMAF was incubated in PBS, human plasma, cynomolgus monkey plasma, mouse plasma, and rat plasma for up to 7 days, and then analyzed by RP-HPLC for DAR values and ELISA for total antibody concentration. Neither drug loss through deconjugation (Figure 9) nor antibody loss through protein degradation (Figure S4) was observed.

DISCUSSION

Using Xpress CF+, an *E. coli* based cell free expression system, we produced six trastuzumab variants with pAMF site-specifically incorporated in V_L, C_H1, and C_H3 domains, respectively. These pAMF containing antibodies enabled efficient conjugation of MMAF, MMAE, and maytansinoid via DBCO-$PEG_{(4)}$ linker. A RP-HPLC assay was developed for DAR characterization, which is versatile for both reduced and intact site-specific ADCs. These Xpress CF+ produced site-specific ADCs possess high DAR values, potent cell killing, and in vitro plasma stability. In addition, we generated a DAR 4 site-specific ADC with MMAF conjugation at both LC and HC, which further improved the cell killing activity.

The Effect of Drug Absorption on Chromatography-Based DAR Determination. All three payloads used in this work have little contribution to absorption at the monitoring wavelength (280 nm), making it feasible to use peak area (or peak height) for DAR determination without any correction for absorbance contributions from the drugs. However, when a payload has a strong absorption at the monitoring wavelength, its impact on relative absorption coefficients of the different DAR species should be considered.

Selection of DAR Characterization Method. The selection of appropriate method(s) for DAR characterization depends on the properties of the ADCs. As the most widely used method for DAR determination, LC-MS is not limited by either the complexity or the linker-drug chemistry of the ADCs, given that the differentiation is based on mass.[36,37] However, the data analysis is generally more complicated and time-consuming. HIC and RP have been applied to ADCs with nonsite-specific conjugation of MMAE on interchain cysteines,[36,45,46] though their use on other heterogeneous ADCs have not been reported yet. Additionally, HIC is the only

DOI: 10.1021/acs.oprd.6b00072
Org. Process Res. Dev. 2016, 20, 1034−1043

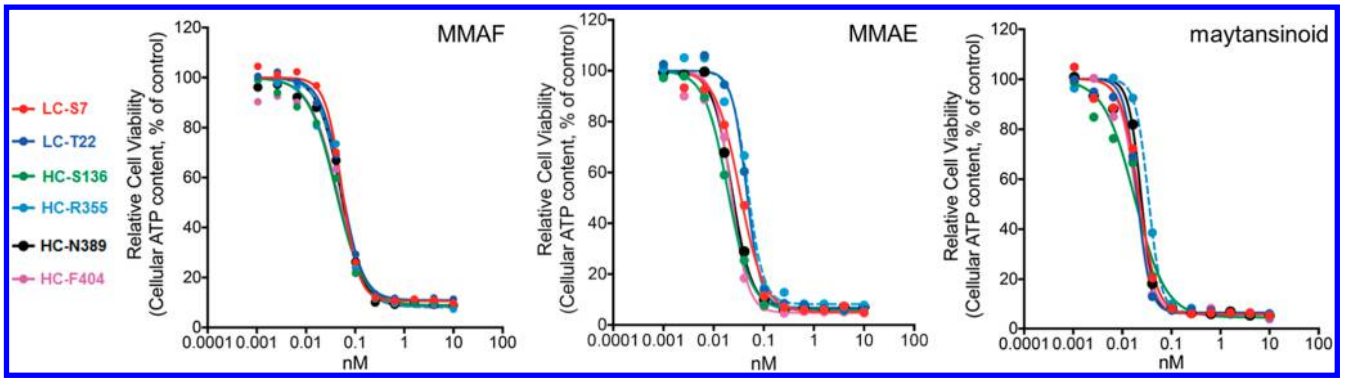

Figure 8. Cell killing of Xpress CF+ produced site-specific ADCs. MMAF, MMAE, and maytansinoid conjugated ADCs showed potent cell killing on SKBR3 cells after 5-day treatment.

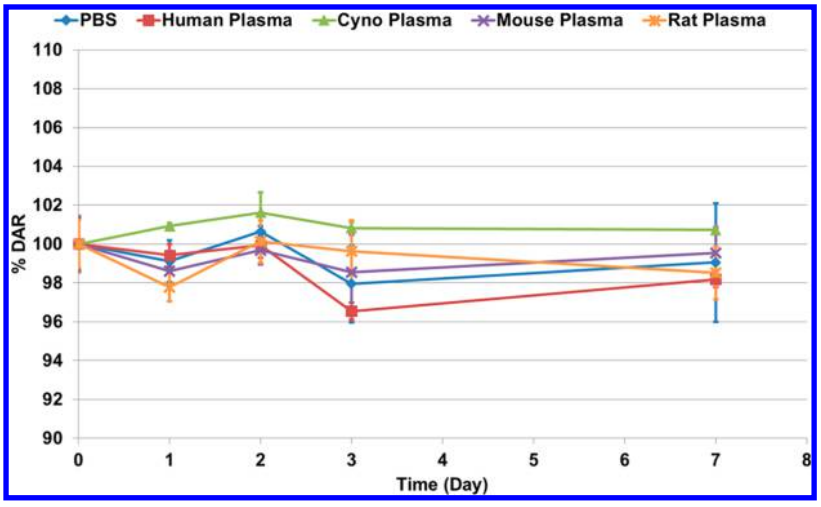

Figure 9. In vitro plasma stability of HC-F404-MMAF. DAR values remained almost unchanged after 7 day incubation in PBS (blue), human plasma (red), cynomolgus plasma (green), mouse (purple), and rat plasma (orange), indicating that the linker-drug on ADC is stable in plasma.

method capable of isolating different species in native conformation for further investigation.[46] RP is compatible with LC-MS to enable high-resolution separation prior to MS analysis.[37] However, as both HIC and RP rely on hydrophobicity difference among species with various levels of conjugation, they may not be suitable for monitoring certain drug conjugations, for instance gemcitabine, the conjugation of which does not introduce a detectable hydrophobicity change (data not shown). Other less commonly used methods may be only applicable in certain circumstances. icIEF based DAR characterization requires that the drug conjugation has impact on the pI of the ADCs.[49] UV/vis spectroscopic analysis relies on the distinguishable difference of A_{max} values of UV/vis spectra between the drug and the antibody.[50] Furthermore, prior to DAR analysis by UV/vis, the excess free drug-linker is required to be removed completely. The applications of all aforementioned methods, which were previously developed for heterogeneous ADCs, can be extrapolated to site-specific ADCs. Apparently, the merits and limitations of these methods are still present in DAR characterization of site-specific ADCs, but the decreasing heterogeneity of site-specific ADCs may loosen the limitation to some extent. For example, contrary to popular practice of applying RP to reduced ADCs to achieve higher resolution, we have demonstrated that RP is also capable of separation of intact site-specific ADCs with 0, 1, and 2 drugs conjugated.

Xpress CF+ ADC Technology Scalability. It is noteworthy that Xpress CF+ system possesses an almost linear scalability, from small scale in 96-well plate (~100 uL), to medium scale in Petri dish, wave bag, or stirred tank reactor (0.5–4 L), to manufacturing scale fermenters.[26,27] Recently, we have successfully performed a 85 L production of pAMF containing mAb1 using Xpress CF+, where the resultant end product had a DAR of over 1.9 after well-established purification and conjugation processes (Sutro proprietary data).

Control of Free Drug. As providing drug in excess is a necessity in order to achieve near complete conjugation, it is critical to remove the remaining unconjugated drug, the presence of which would complicate the efficacy and safety profiles of the ADC product. A common practice is to implement additional purification steps after conjugation to remove the free drugs such as gel filtration at laboratory scale or tangential flow filtration (TFF) at manufacturing scale. Meanwhile, appropriate analytical method(s) need to be in place to identify, characterize, and control any residual free drug that is not completely removed by the purification effort.[55−58] Due to its outstanding sensitivity and precision, RP-HPLC assays are a commonly used platform for free drug assay development.[36] For example, quantification of free drug can be achieved on a HISEP column with direct injection of ADCs containing free drug.[59]

DOI: 10.1021/acs.oprd.6b00072
Org. Process Res. Dev. 2016, 20, 1034−1043

■ ASSOCIATED CONTENT

Supporting Information

The Supporting Information is available free of charge on the ACS Publications website at DOI: 10.1021/acs.oprd.6b00072.

Reduced RP-HPLC chromatograms for DAR determination, RP-HPLC chromatograms of MMAE, and maytansinoid site-specific ADCs, intact RP-HPLC chromatograms of MMAF site-specific ADCs, pharmacokinetics of site-specific ADCs in plasma, table of intact mass of fully conjugated ADCs observed in LC-MS (PDF)

■ AUTHOR INFORMATION

Corresponding Author

*E-mail: gyin@sutrobio.com.

Notes

The authors declare no competing financial interest.

■ ABBREVIATIONS

ADC, antibody drug conjugate; nnAA, non-natural amino acid; pAMF, *para*-azidomethyl-L-phenylalanine; DBCO-$(PEG)_4$, dibenzocyclooctyl-(polyethylene glycol)$_4$; RP-HPLC, reversed-phase high-performance liquid chromatography; DAR, drug to antibody ratio; LC, immunoglobulin light chain; HC, immunoglobulin heavy chain; LC-MS, liquid chromatography mass spectrometry; MMAF, monomethyl auristatin F; MMAE, monomethyl auristatin E

■ REFERENCES

(1) LoRusso, P. M.; Weiss, D.; Guardino, E.; Girish, S.; Sliwkowski, M. X. *Clin. Cancer Res.* **2011**, *17* (20), 6437−6447.

(2) Katz, J.; Janik, J. E.; Younes, A. *Clin. Cancer Res.* **2011**, *17* (20), 6428−6436.

(3) Senter, P. D.; Sievers, E. L. *Nat. Biotechnol.* **2012**, *30* (7), 631−637.

(4) Behrens, C. R.; Liu, B. *MAbs* **2014**, *6* (1), 46−53.

(5) Panowski, S.; Bhakta, S.; Raab, H.; Polakis, P.; Junutula, J. R. *MAbs* **2014**, *6* (1), 34−45.

(6) Xu, K.; Liu, L.; Dere, R.; Mai, E.; Hendricks, A.; Lin, K.; Junutula, J. R.; Kaur, S. *Bioanalysis* **2013**, *5* (9), 1057−1071.

(7) Hamblett, K. J.; Senter, P. D.; Chace, D. F.; Sun, M. M. C.; Lenox, J.; Cerveny, C. G.; Kissler, K. M.; Bernhardt, S. X.; Kopcha, A. K.; Zabinski, R. F.; Meyer, D. L.; Francisco, J. a. *Clin. Cancer Res.* **2004**, *10* (425), 7063−7070.

(8) Wang, L.; Amphlett, G.; Blättler, W. A.; Lambert, J. M.; Zhang, W. *Protein Sci.* **2005**, *14* (9), 2436−2446.

(9) Kline, T.; Steiner, A. R.; Penta, K.; Sato, A. K.; Hallam, T. J.; Yin, G. *Pharm. Res.* **2015**, *32* (11), 3480−3493.

(10) Junutula, J. R.; Flagella, K. M.; Graham, R. a.; Parsons, K. L.; Ha, E.; Raab, H.; Bhakta, S.; Nguyen, T.; Dugger, D. L.; Li, G.; Mai, E.; Phillips, G. D. L.; Hiraragi, H.; Fuji, R. N.; Tibbitts, J.; Vandlen, R.; Spencer, S. D.; Scheller, R. H.; Polakis, P.; Sliwkowski, M. X. *Clin. Cancer Res.* **2010**, *16* (19), 4769−4778.

(11) Bender, B.; Leipold, D. D.; Xu, K.; Shen, B.-Q.; Tibbitts, J.; Friberg, L. E. *AAPS J.* **2014**, *16* (5), 994−1008.

(12) Pillow, T. H.; Tien, J.; Parsons-reponte, K. L.; Bhakta, S.; Li, H.; Staben, L. R.; Li, G.; Chuh, J.; Donohue, A. F.; Darwish, M.; Yip, V.; Liu, L.; Leipold, D. D.; Su, D.; Wu, E.; Spencer, S. D.; Shen, B.; Xu, K.; Kozak, K. R.; Raab, H.; Vandlen, R.; Phillips, G. D. L.; Scheller, R. H.; Polakis, P.; Sliwkowski, M. X.; Flygare, J. A.; Junutula, J. R. *J. Med. Chem.* **2014**, *57* (19), 7890−7899.

(13) Jackson, D.; Atkinson, J.; Guevara, C. I.; Zhang, C.; Kery, V.; Moon, S. J.; Virata, C.; Yang, P.; Lowe, C.; Pinkstaff, J.; Cho, H.; Knudsen, N.; Manibusan, A.; Tian, F.; Sun, Y.; Lu, Y.; Sellers, A.; Jia, X. C.; Joseph, I.; Anand, B.; Morrison, K.; Pereira, D. S.; Stover, D. *PLoS One* **2014**, *9* (1), 0083865.

(14) Hallam, T. J.; Smider, V. V. *Future Med. Chem.* **2014**, *6* (11), 1309−1324.

(15) Axup, J. Y.; Bajjuri, K. M.; Ritland, M.; Hutchins, B. M.; Kim, C. H.; Kazane, S. a.; Halder, R.; Forsyth, J. S.; Santidrian, a. F.; Stafin, K.; Lu, Y.; Tran, H.; Seller, a. J.; Biroc, S. L.; Szydlik, a.; Pinkstaff, J. K.; Tian, F.; Sinha, S. C.; Felding-Habermann, B.; Smider, V. V.; Schultz, P. G. *Proc. Natl. Acad. Sci. U. S. A.* **2012**, *109* (40), 16101−16106.

(16) Chin, J. W.; Santoro, S. W.; Martin, A. B.; King, D. S.; Wang, L.; Schultz, P. G. *J. Am. Chem. Soc.* **2002**, *124* (31), 9026−9027.

(17) Zimmerman, E. S.; Heibeck, T. H.; Gill, A.; Li, X.; Murray, C. J.; Madlansacay, M. R.; Tran, C.; Uter, N. T.; Yin, G.; Rivers, P. J.; Yam, A. Y.; Wang, W. D.; Steiner, A. R.; Bajad, S. U.; Penta, K.; Yang, W.; Hallam, T. J.; Thanos, C. D.; Sato, A. K. *Bioconjugate Chem.* **2014**, *25* (2), 351−361.

(18) Nguyen, D. P.; Lusic, H.; Neumann, H.; Kapadnis, P. B.; Deiters, A.; Chin, J. W. *J. Am. Chem. Soc.* **2009**, *131* (25), 8720−8721.

(19) Strop, P.; Liu, S. H.; Dorywalska, M.; Delaria, K.; Dushin, R. G.; Tran, T. T.; Ho, W. H.; Farias, S.; Casas, M. G.; Abdiche, Y.; Zhou, D.; Chandrasekaran, R.; Samain, C.; Loo, C.; Rossi, A.; Rickert, M.; Krimm, S.; Wong, T.; Chin, S. M.; Yu, J.; Dilley, J.; Chaparro-Riggers, J.; Filzen, G. F.; O'Donnell, C. J.; Wang, F.; Myers, J. S.; Pons, J.; Shelton, D. L.; Rajpal, A. *Chem. Biol.* **2013**, *20* (2), 161−167.

(20) Agarwal, P.; van der Weijden, J.; Sletten, E. M.; Rabuka, D.; Bertozzi, C. R. *Proc. Natl. Acad. Sci. U. S. A.* **2013**, *110* (1), 46−51.

(21) Zhu, Z.; Ramakrishnan, B.; Li, J.; Wang, Y.; Feng, Y.; Prabakaran, P.; Colantonio, S.; Dyba, M. A.; Qasba, P. K.; Dimitrov, D. S. *MAbs* **2014**, *6* (5), 1190−1200.

(22) Zhou, Q.; Stefano, J. E.; Manning, C.; Kyazike, J.; Chen, B.; Gianolio, D. A.; Park, A.; Busch, M.; Bird, J.; Zheng, X.; Simonds-Mannes, H.; Kim, J.; Gregory, R. C.; Miller, R. J.; Brondyk, W. H.; Dhal, P. K.; Pan, C. Q. *Bioconjugate Chem.* **2014**, *25* (3), 510−520.

(23) Jackson, D. Y.; Ha, E. Antibody-drug conjugates and related compounds, compositions, and methods. WO 2013085925 A1, June 13, 2013.

(24) Robin, M. P.; Mabire, A. B.; Damborsky, J. C.; Thom, E. S.; Winzer-Serhan, U. H.; Raymond, J. E.; O'Reilly, R. K. *J. Am. Chem. Soc.* **2013**, *135* (25), 9518−9524.

(25) Badescu, G.; Bryant, P.; Bird, M.; Henseleit, K.; Swierkosz, J.; Parekh, V.; Tommasi, R.; Pawlisz, E.; Jurlewicz, K.; Farys, M.; Camper, N.; Sheng, X.; Fisher, M.; Grygorash, R.; Kyle, A.; Abhilash, A.; Frigerio, M.; Edwards, J.; Godwin, A. *Bioconjugate Chem.* **2014**, *25* (6), 1124−1136.

(26) Yin, G.; Garces, E. D.; Yang, J.; Zhang, J.; Tran, C.; Steiner, A. R.; Roos, C.; Bajad, S.; Hudak, S.; Penta, K.; Zawada, J.; Pollitt, S.; Murray, C. J. *MAbs* **2012**, *4* (2), 217−225.

(27) Zawada, J. F.; Yin, G.; Steiner, A. R.; Yang, J.; Naresh, A.; Roy, S. M.; Gold, D. S.; Heinsohn, H. G.; Murray, C. J. *Biotechnol. Bioeng.* **2011**, *108* (7), 1570−1578.

(28) Xu, Y.; Lee, J.; Tran, C.; Heibeck, T. H.; Wang, W. D.; Yang, J.; Stafford, R. L.; Steiner, A. R.; Sato, A. K.; Hallam, T. J.; Yin, G. *MAbs* **2015**, *7* (1), 231−242.

(29) Thanos, C. D.; Mcevoy, L.; Yin, G.; Penta, K.; Baliga, R.; Bajad, S.; Pollitt, S.; Murray, C.; Steiner, A. R.; Gill, A. Antibodies comprising site-specific non-natural amino acid residues, methods of their preparation and methods of their use. WO 2013185115A1, 2013.

(30) Young, T. S.; Ahmad, I.; Yin, J. a.; Schultz, P. G. *J. Mol. Biol.* **2010**, *395* (2), 361−374.

(31) Johnson, D. B. F.; Xu, J.; Shen, Z.; Takimoto, J. K.; Schultz, M. D.; Schmitz, R. J.; Xiang, Z.; Ecker, J. R.; Briggs, S. P.; Wang, L. *Nat. Chem. Biol.* **2011**, *7* (11), 779−786.

(32) Loscha, K. V.; Herlt, A. J.; Qi, R.; Huber, T.; Ozawa, K.; Otting, G. *Angew. Chem., Int. Ed.* **2012**, *51* (9), 2243−2246.

(33) Hong, S. H.; Ntai, I.; Haimovich, A. D.; Kelleher, N. L.; Isaacs, F. J.; Jewett, M. C. *ACS Synth. Biol.* **2014**, *3* (6), 398−409.

(34) Agafonov, D. E.; Huang, Y.; Grote, M.; Sprinzl, M. *FEBS Lett.* **2005**, *579* (10), 2156−2160.

DOI: 10.1021/acs.oprd.6b00072
Org. Process Res. Dev. 2016, 20, 1034−1043

(35) Lee, K. B.; Kim, H.-C.; Kim, D.-M.; Kang, T. J.; Suga, H. *J. Biotechnol.* **2013**, *164* (2), 330−335.
(36) Wakankar, A.; Chen, Y.; Gokarn, Y.; Jacobson, F. S. *MAbs* **2011**, *3* (2), 161−172.
(37) Basa, L. *Methods Mol. Biol.* **2013**, *1045*, 285−293.
(38) Beck, A.; Terral, G.; Debaene, F.; Wagner-Rousset, E.; Marcoux, J.; Janin-Bussat, M.-C.; Colas, O.; Van Dorsselaer, A.; Cianférani, S. *Expert Rev. Proteomics* **2016**, *13* (2), 157−183.
(39) Quiles, S.; Raisch, K. P.; Sanford, L. L.; Bonner, J. A.; Safavy, A. *J. Med. Chem.* **2010**, *53* (2), 586−594.
(40) Safavy, A.; Bonner, J. A.; Waksal, H. W.; Buchsbaum, D. J.; Gillespie, G. Y.; Khazaeli, M. B.; Arani, R.; Chen, D.-T.; Carpenter, M.; Raisch, K. P. *Bioconjugate Chem.* **2003**, *14* (2), 302−310.
(41) Siegel, M. M.; Hollander, I. J.; Hamann, P. R.; James, J. P.; Hinman, L.; Smith, B. J.; Farnsworth, A. P.; Phipps, A.; King, D. J.; Karas, M. *Anal. Chem.* **1991**, *63* (21), 2470−2481.
(42) Valliere-Douglass, J. F.; McFee, W. A.; Salas-Solano, O. *Anal. Chem.* **2012**, *84* (6), 2843−2849.
(43) Rodriguez-Aller, M.; Guillarme, D.; Beck, A.; Fekete, S. *J. Pharm. Biomed. Anal.* **2016**, *118*, 393−403.
(44) Cusumano, A.; Guillarme, D.; Beck, A.; Fekete, S. *J. Pharm. Biomed. Anal.* **2016**, *121*, 161−173.
(45) Ouyang, J. *Methods Mol. Biol.* **2013**, *1045*, 275−283.
(46) Haverick, M.; Mengisen, S.; Shameem, M.; Ambrogelly, A. *MAbs* **2014**, *6* (4), 852−858.
(47) McDonagh, C. F.; Turcott, E.; Westendorf, L.; Webster, J. B.; Alley, S. C.; Kim, K.; Andreyka, J.; Stone, I.; Hamblett, K. J.; Francisco, J. a.; Carter, P. *Protein Eng., Des. Sel.* **2006**, *19* (7), 299−307.
(48) Sun, M. M. C.; Beam, K. S.; Cerveny, C. G.; Hamblett, K. J.; Blackmore, R. S.; Torgov, M. Y.; Handley, F. G. M.; Ihle, N. C.; Senter, P. D.; Alley, S. C. *Bioconjugate Chem.* **2005**, *16* (5), 1282−1290.
(49) Lin, J.; Lazar, A. C. *Methods Mol. Biol.* **2013**, *1045*, 295−302.
(50) Chen, Y. *Methods Mol. Biol.* **2013**, *1045*, 267−273.
(51) Groff, D.; Armstrong, S.; Rivers, P. J.; Zhang, J.; Yang, J.; Green, E.; Rozzelle, J.; Liang, S.; Kittle, J. D.; Steiner, A. R.; Baliga, R.; Thanos, C. D.; Hallam, T. J.; Sato, A. K.; Yam, A. Y. *MAbs* **2014**, *6* (3), 671−678.
(52) Cai, Q.; Hanson, J. a.; Steiner, A. R.; Tran, C.; Masikat, M. R.; Chen, R.; Zawada, J. F.; Sato, A. K.; Hallam, T. J.; Yin, G. *Biotechnol. Prog.* **2015**, *31* (3), 823−831.
(53) Jewett, J. C.; Bertozzi, C. R. *Chem. Soc. Rev.* **2010**, *39* (4), 1272−1279.
(54) Strop, P.; Delaria, K.; Foletti, D.; Witt, J. M.; Hasa-Moreno, A.; Poulsen, K.; Casas, M. G.; Dorywalska, M.; Farias, S. E.; Pios, A.; Lui, V.; Dushin, R. G.; Zhou, D.; Navaratnam, T.; Tran, T.-T.; Sutton, J.; Lindquist, K. C.; Liu, S.-H.; Shelton, D. L.; Pons, J.; Rajpal, A. *Nat. Biotechnol.* **2015**, *33* (7), 694−696.
(55) Birdsall, R. E.; McCarthy, S. M.; Janin-Bussat, M. C.; Perez, M.; Haeuw, J.-F.; Chen, W.; Beck, A. *MAbs* **2016**, *8* (2), 306−317.
(56) Li, Y.; Gu, C.; Gruenhagen, J.; Yehl, P.; Chetwyn, N. P.; Medley, C. D. *MAbs* **2016**, *8*, 698−705.
(57) Li, Y.; Gu, C.; Gruenhagen, J.; Zhang, K.; Yehl, P.; Chetwyn, N. P.; Medley, C. D. *J. Chromatogr. A* **2015**, *1393*, 81−88.
(58) Chen, T.; Su, D.; Gruenhagen, J.; Gu, C.; Li, Y.; Yehl, P.; Chetwyn, N. P.; Medley, C. D. *J. Pharm. Biomed. Anal.* **2016**, *117*, 304−310.
(59) Fleming, M. S.; Zhang, W.; Lambert, J. M.; Amphlett, G. *Anal. Biochem.* **2005**, *340* (2), 272−278.
(60) Saphire, E. O.; Parren, P. W.; Pantophlet, R.; Zwick, M. B.; Morris, G. M.; Rudd, P. M.; Dwek, R. A.; Stanfield, R. L.; Burton, D. R.; Wilson, I. A. *Science* **2001**, *293* (5532), 1155−1159.

DOI: 10.1021/acs.oprd.6b00072
Org. Process Res. Dev. 2016, 20, 1034−1043